Electronic Supplementary Material (ESI) for New Journal of Chemistry.
This journal is © The Royal Society of Chemistry and the Centre National de la Recherche Scientifique 2017

Supporting Information

Two Luminescent Zn(II)/Cd(II) Metal-Organic Frameworks as Rare Multifunctional Sensors

Jinfang Zhang*, Linpei Gong, Jiaoyang Feng, Junjie Wu, Chi Zhang*

China-Australia Joint Research Center for Functional Molecular Materials,School of Chemical and Material Engineering, Jiangnan University, Wuxi 214122, P.R. China

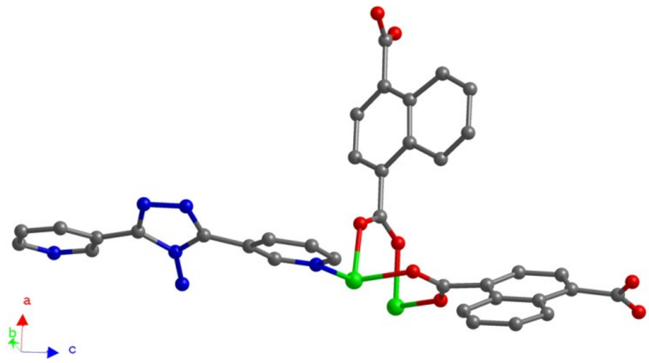

Figure S1. View of the asymmetric unit of **1** (two DMF had been squeezed because of their disorder; C grey, N blue, O red, Zn green and all H atoms are omitted for clarity).

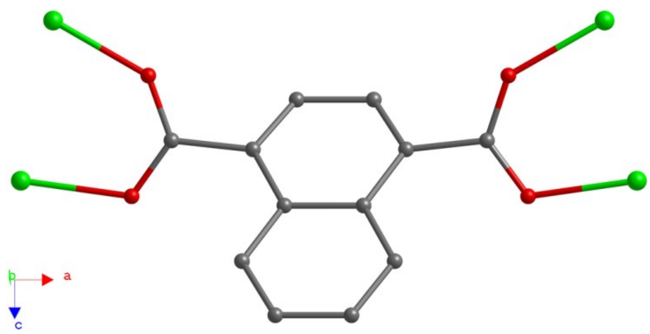

Figure S2. Coordination environments of 1,4-ndc in **1** (C grey, O red, Zn green and all H atoms are omitted for clarity).

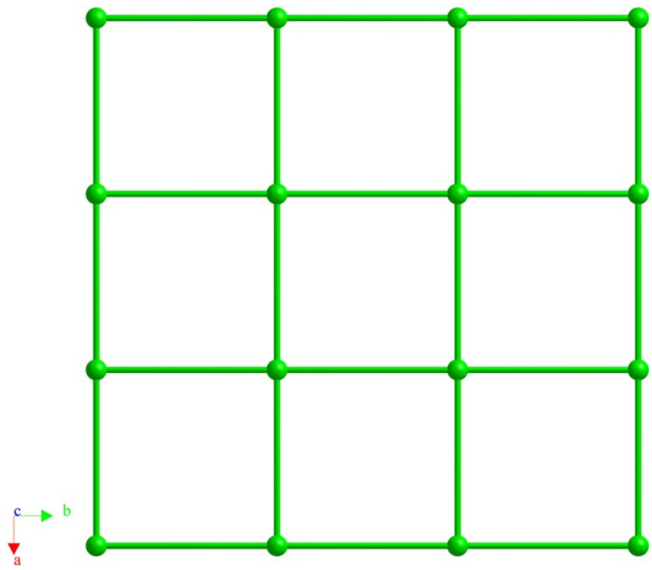

Figure S3. View of the ($4^4.6^2$) topology of **1**.

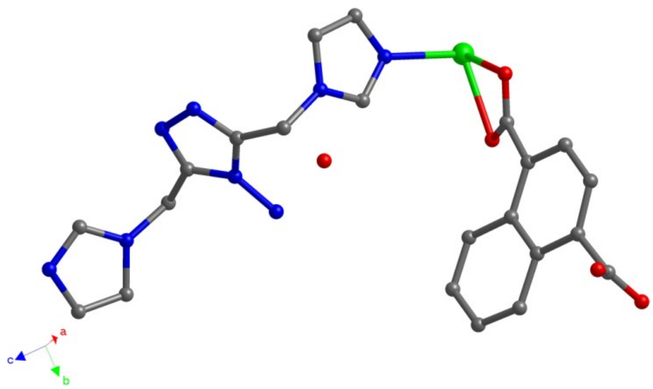

Figure S4.View of the asymmetric unit of **2** (C grey, N blue, O red, Cd green and all H atoms are omitted for clarity).

Figure S5. Coordination environments of 1,4-ndc in**2**(C grey, O red, Cd green and all H atoms are omitted for clarity).

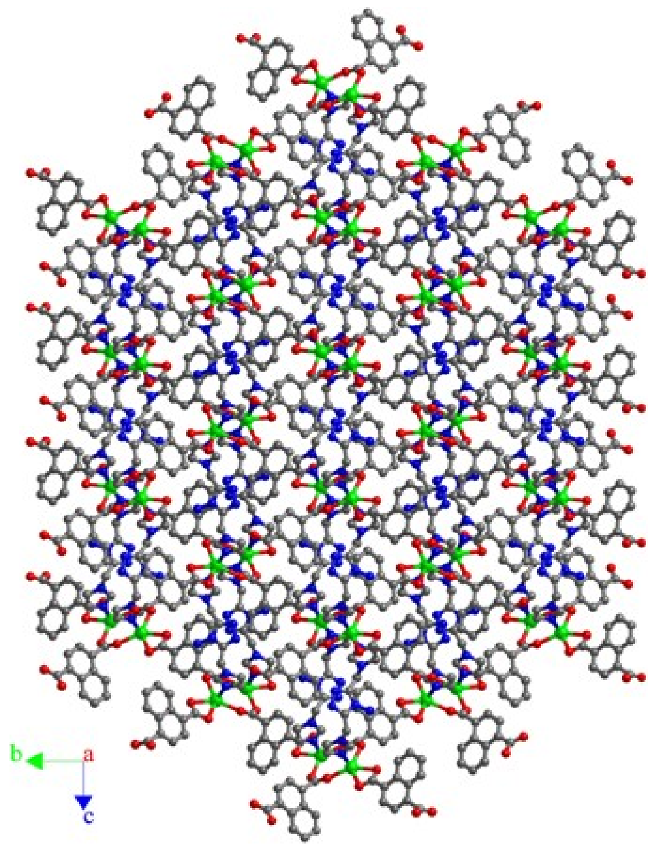

Figure S6. View of a3-D structure of **2** alongthe a-axis(C grey, N blue, O red, Cd green and all H atoms are omitted for clarity).

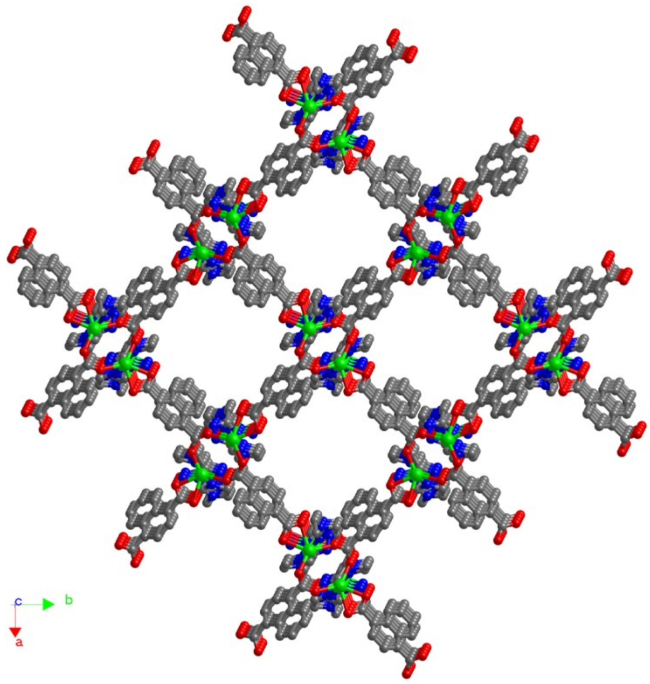

Figure S7. View of a 3-D structure of **2**alongthe c-axis (C grey, N blue, O red, Cd green and all H atoms are omitted for clarity).

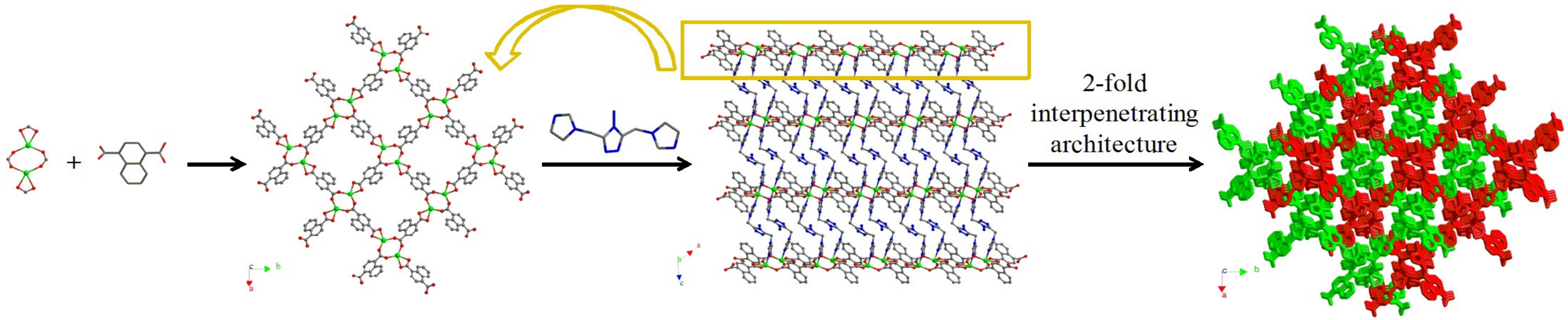

Scheme S1. Illustrative assembly of **2**(C grey, N blue, O red,Cd green and all H atoms being omitted for clarity).

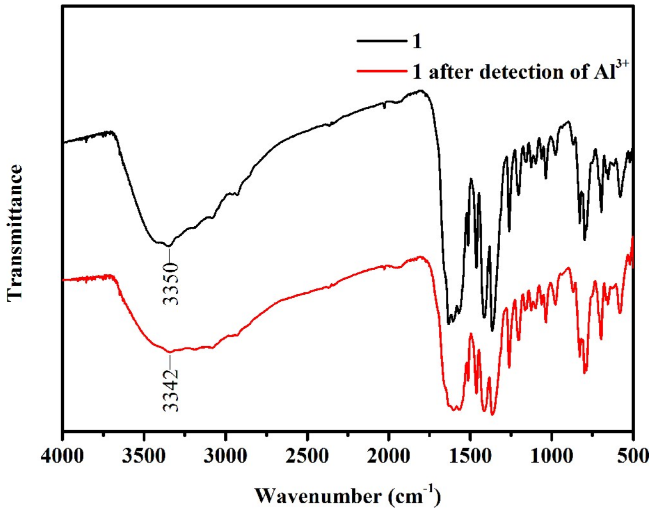

Figure S8. IR spectra of **1** and that after detection of Al^{3+}.

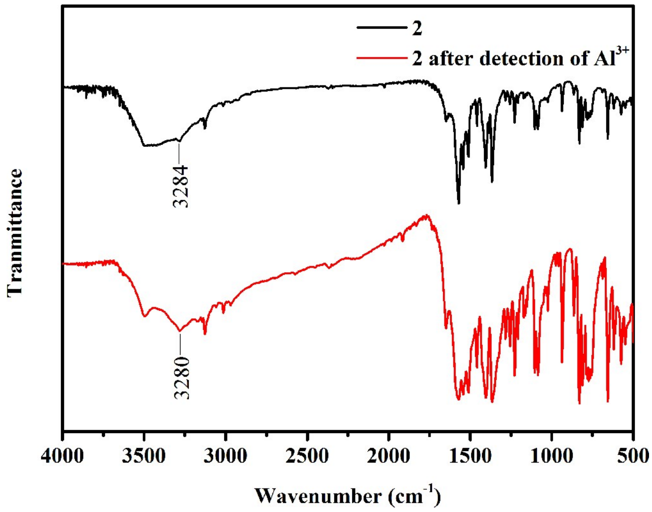

Figure S9. IR spectra of **2** and that after detection of Al^{3+}.

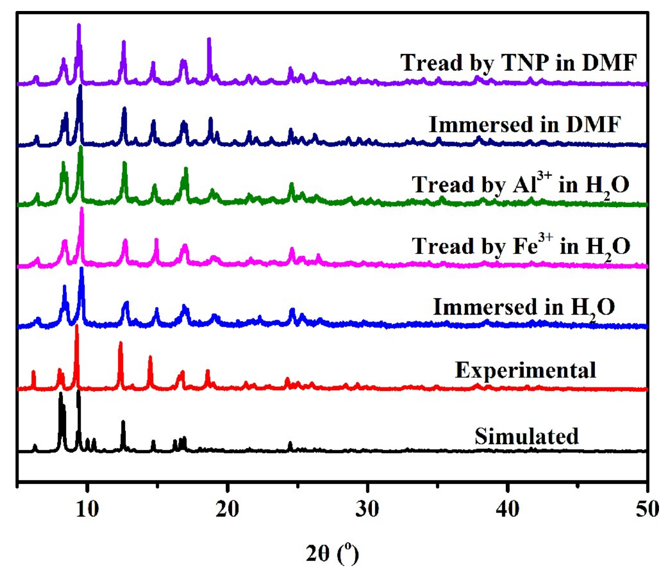

Figure S10.PXRD patterns of **1**.

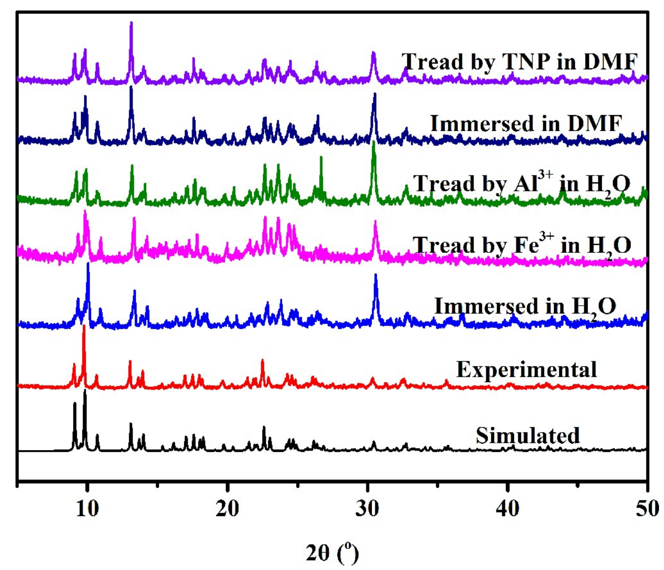

Figure S11.PXRD patterns of **2**.

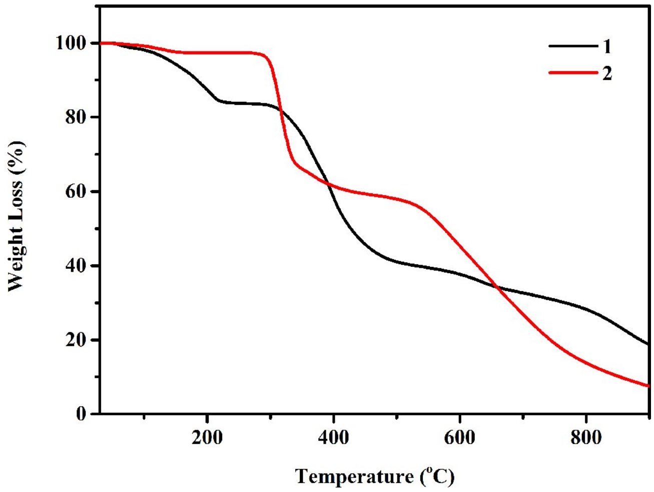

Figure S12. Thermogravimetric analysis of **1** and **2**.

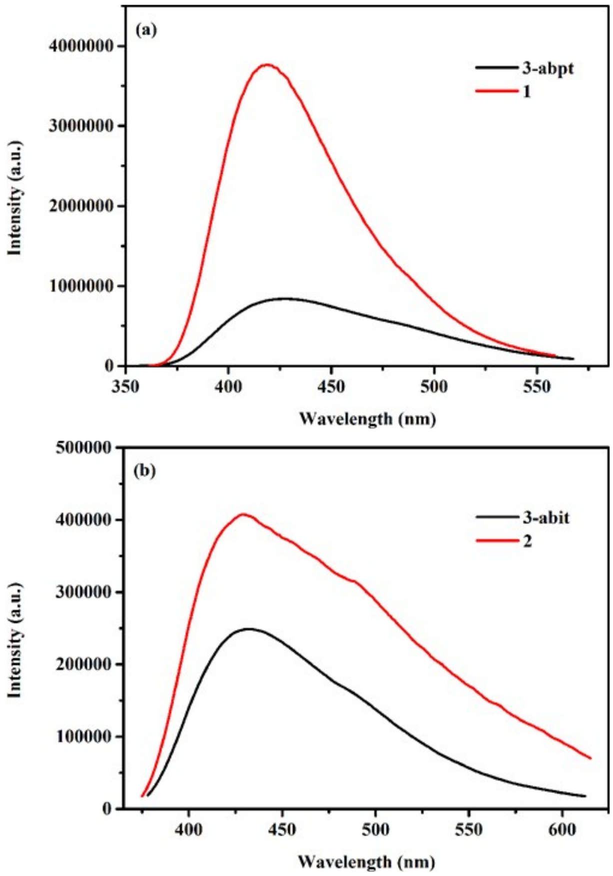

Figure S13. Solid-state emission spectra of the MOFs and the free organic ligands (λ_{ex} = 343 nm for **1** and 3-abpt; λ_{ex} = 350 nm for **2** and 3-abit).

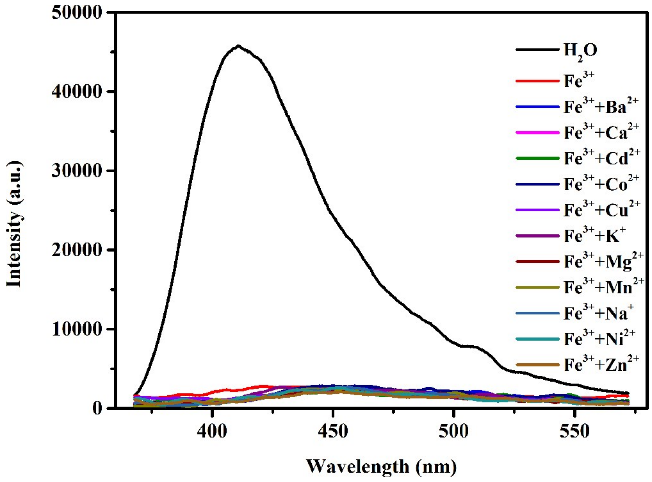

Figure S14. Emission spectra for **1** in aqueous solutions of different metal ions. The concentration of Fe^{3+} and other metal cations was 1×10^{-2} M, respectively (λ_{ex} = 343 nm).

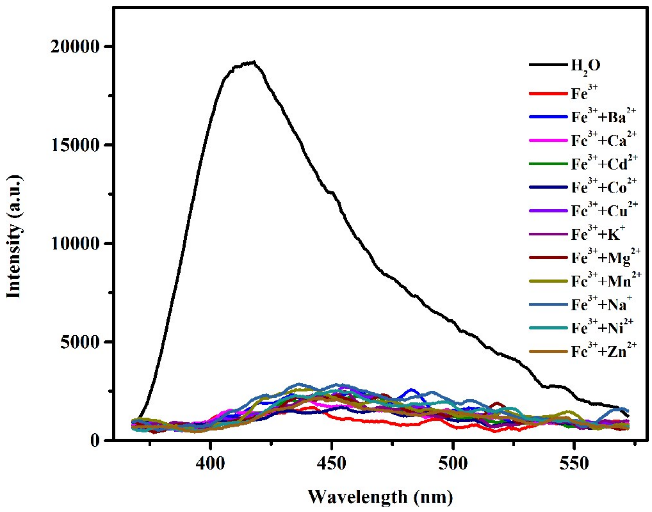

Figure S15. Emission spectra for **2** in aqueous solutions of different metal ions. The concentration of Fe^{3+} and other metal cations was 1×10^{-2} M, respectively (λ_{ex} = 350 nm).

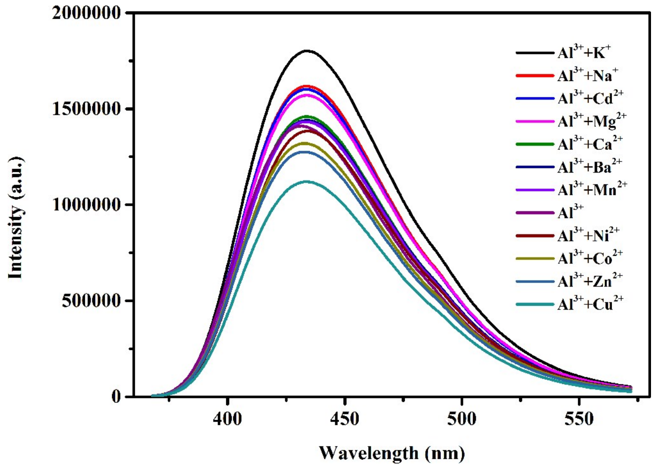

Figure S16. Emission spectra for **1** in aqueous solutions of different metal ions. The concentration of Al^{3+} and other metal cations was 1 ×10^{-2} M, respectively (λ_{ex} = 343 nm).

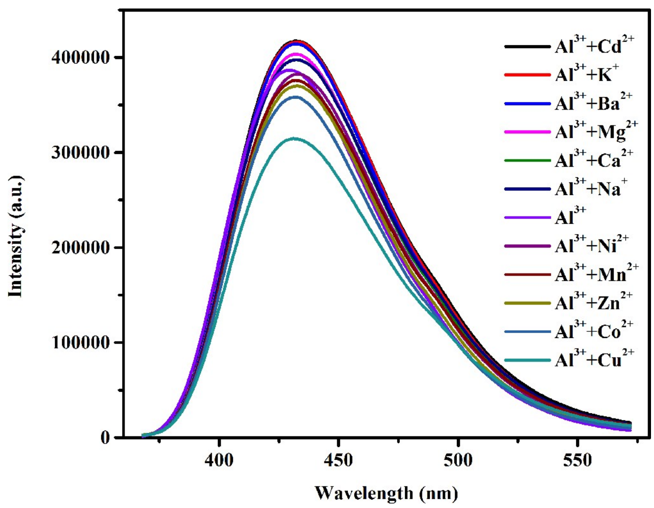

Figure S17. Emission spectra for **2** in aqueous solutions of different metal ions. The concentration of Al^{3+} and other metal cations was 1 ×10^{-2} M, respectively (λ_{ex} = 350 nm).

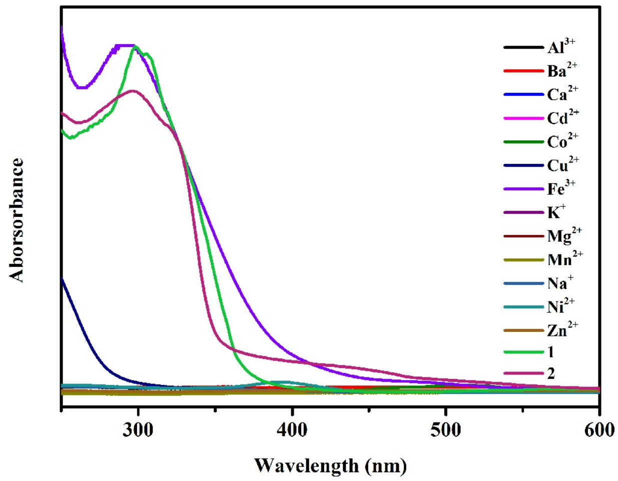

Figure S18. Uv-vis absorption spectra of different metal cations in aqueous solutions and **1-2** in the solid state.

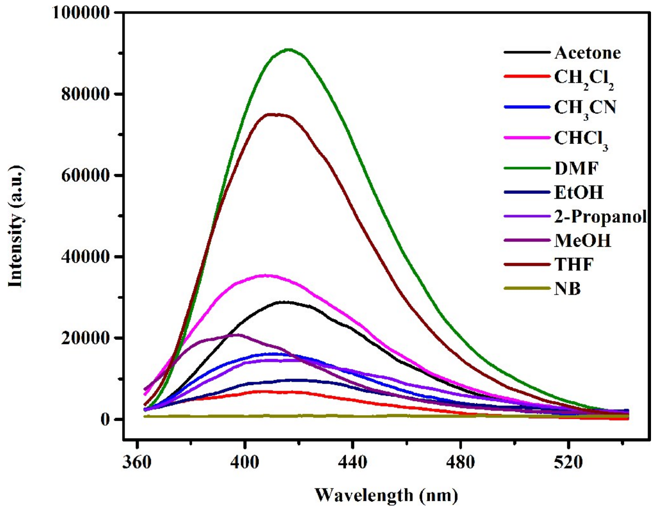

Figure S19. Emission spectra of **1**in different organic dispersants (λ_{ex} = 343 nm).

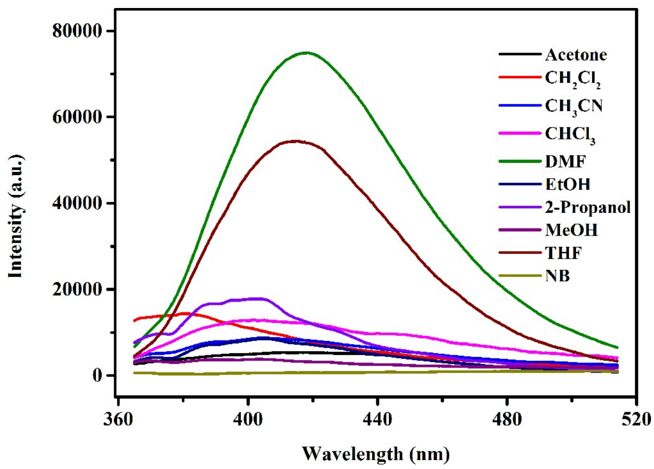

Figure S20. Emission spectra of **2**in different organic dispersants (λ_{ex} = 350 nm).

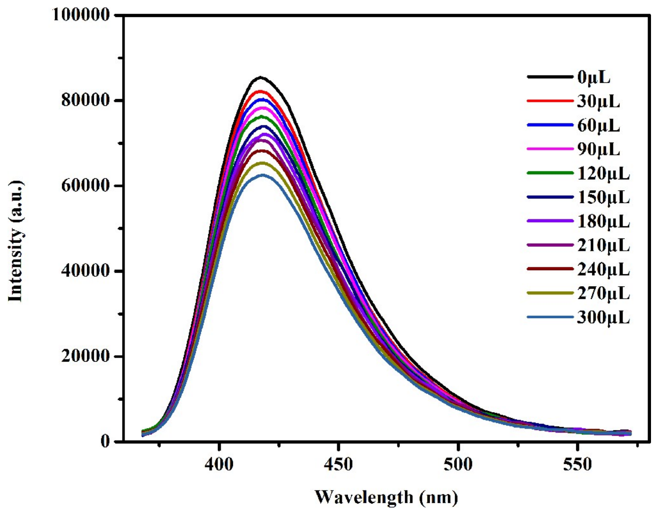

Figure S21. Emission spectra of **1** dispersed in DMF with the addition of different volume of 5mMDMF solution of NB(λ_{ex} = 343 nm).

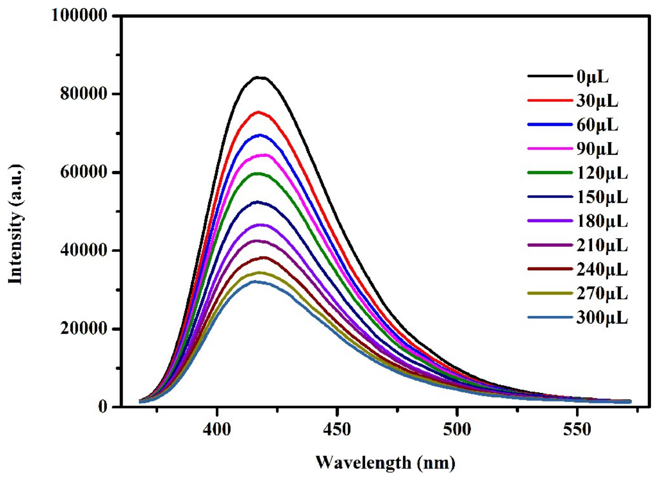

Figure S22. Emission spectra of **1** dispersed in DMF with the addition of different volume of 5mMDMF solution of *m*-DNB(λ_{ex} = 343 nm).

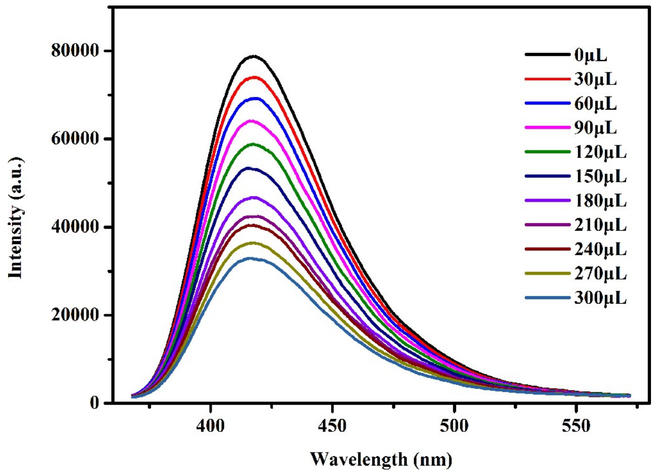

Figure S23. Emission spectra of **1** dispersed in DMF with the addition of different volume of 5mMDMF solution of 2,4-DNT(λ_{ex} = 343 nm).

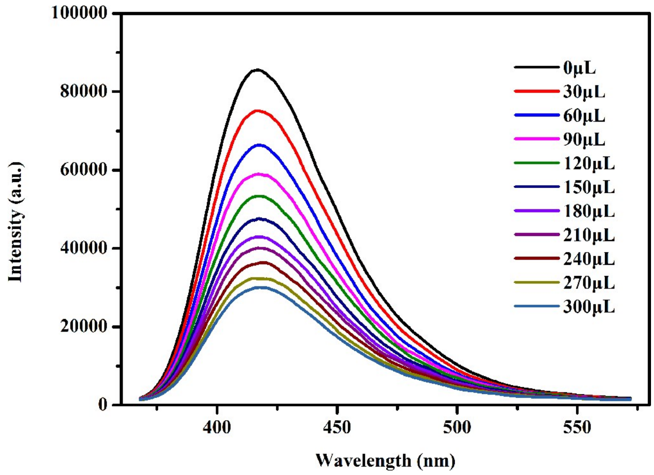

Figure S24. Emission spectra of **1** dispersed in DMF with the addition of different volume of 5mMDMF solution of PNT(λ_{ex} = 343 nm).

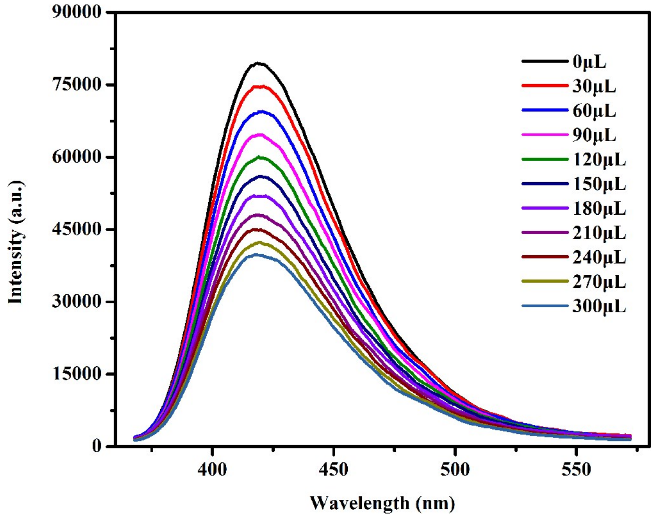

Figure S25. Emission spectra of **2**dispersed in DMF with the addition of different volume of 5mMDMF solution of NB(λ_{ex} = 350 nm).

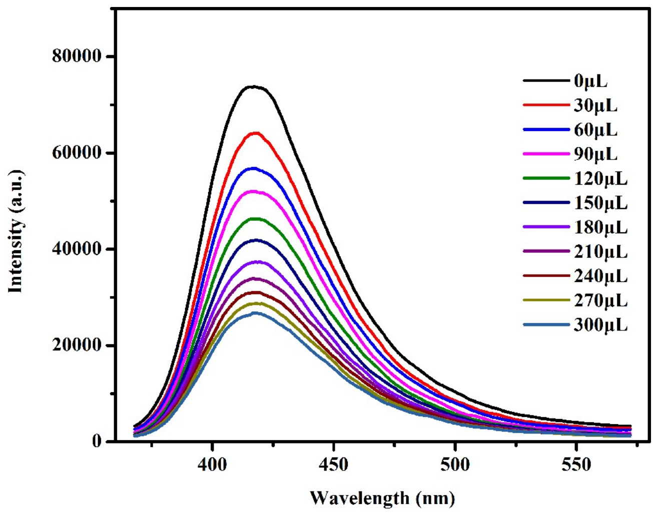

Figure S26. Emission spectra of **2**dispersed in DMF with the addition of different volume of 5mMDMF solution of *m*-DNB(λ_{ex} = 350 nm).

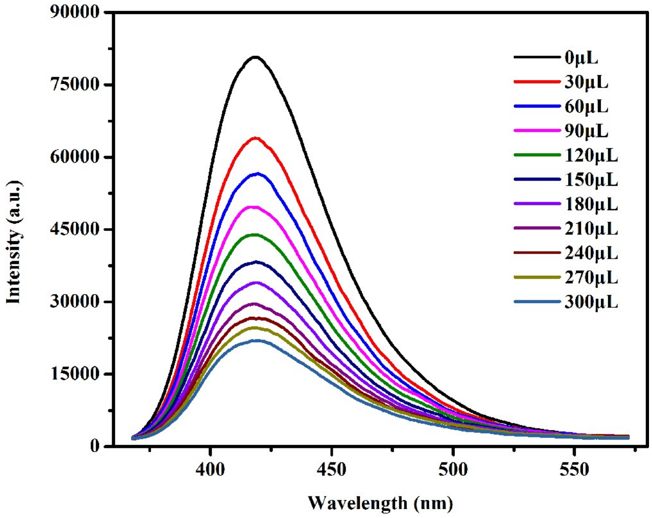

Figure S27. Emission spectra of **2**dispersed in DMF with the addition of different volume of 5mMDMF solution of 2,4-DNT(λ_{ex} = 350 nm).

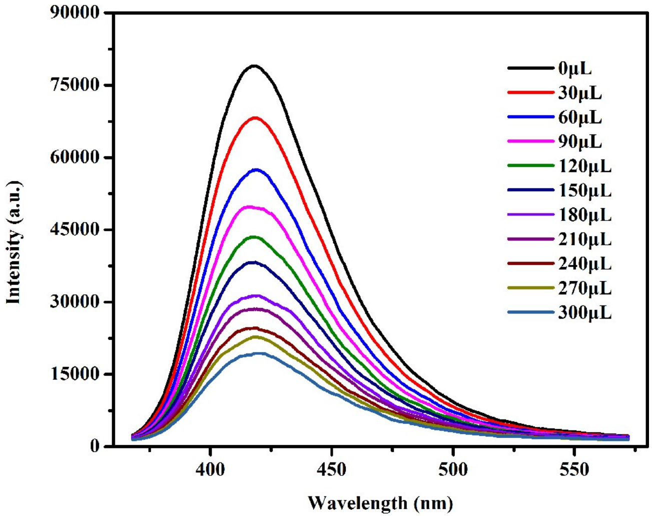

Figure S28. Emission spectra of **2**dispersed in DMF with the addition of different volume of 5mMDMF solution of PNT(λ_{ex} = 350 nm).

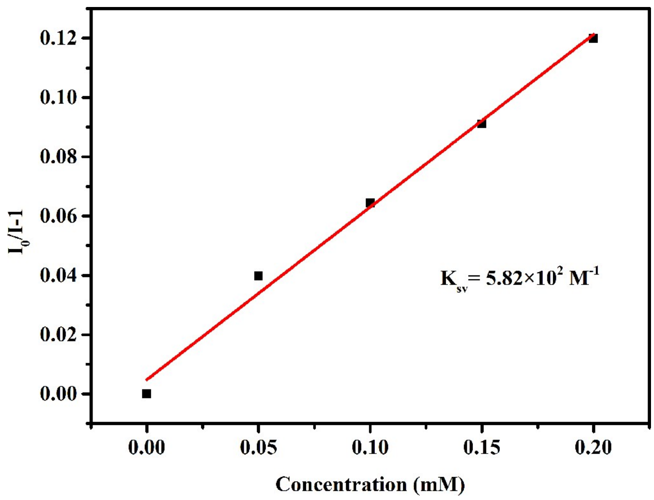

Figure S29. Stern-Volmer plot for NB of **1** in DMF suspension at the low concentration(0-0.2mM).

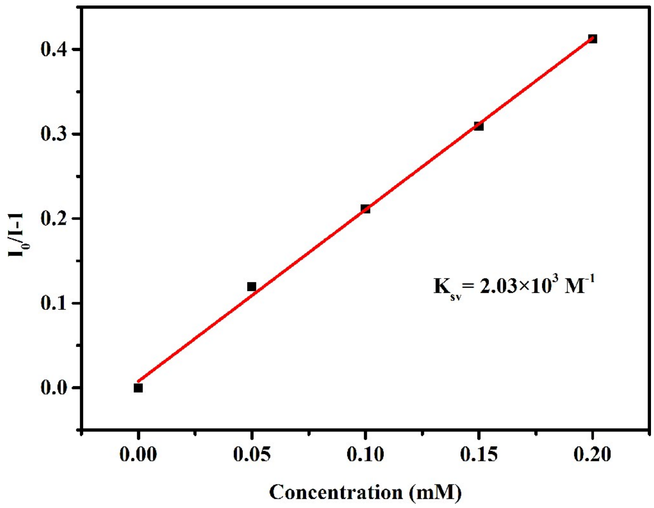

Figure S30. Stern-Volmer plot for *m*-DNB of **1** in DMF suspension at the low concentration(0-0.2mM).

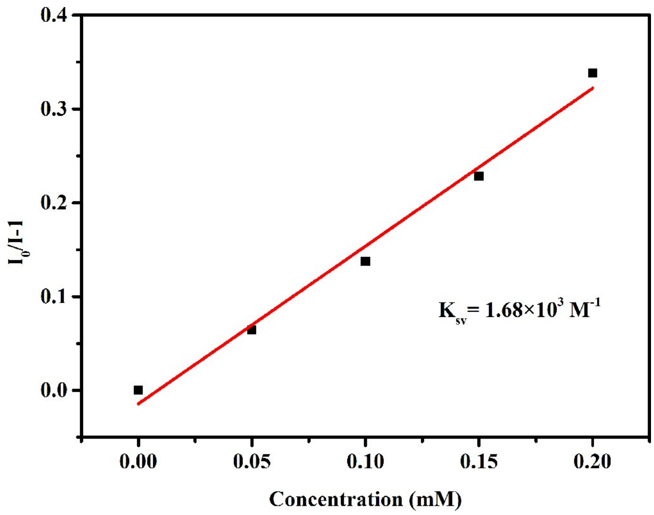

Figure S31. Stern-Volmer plot for 2,4-DNT of **1** in DMF suspension at the low concentration(0-0.2mM).

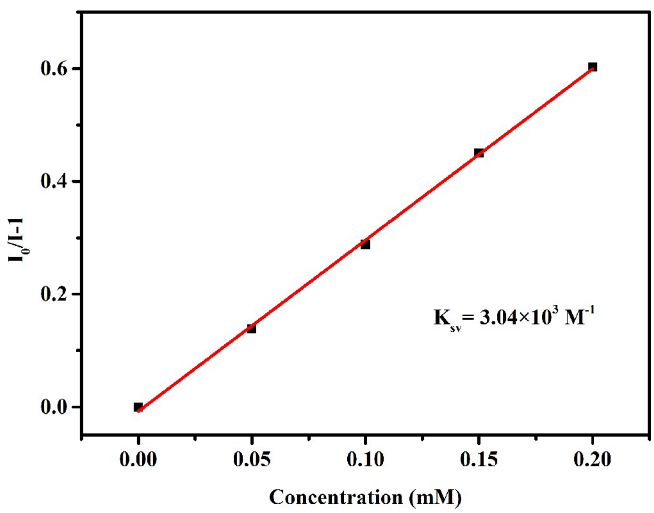

Figure S32. Stern-Volmer plot for PNT of **1** in DMF suspension at the low concentration(0-0.2mM).

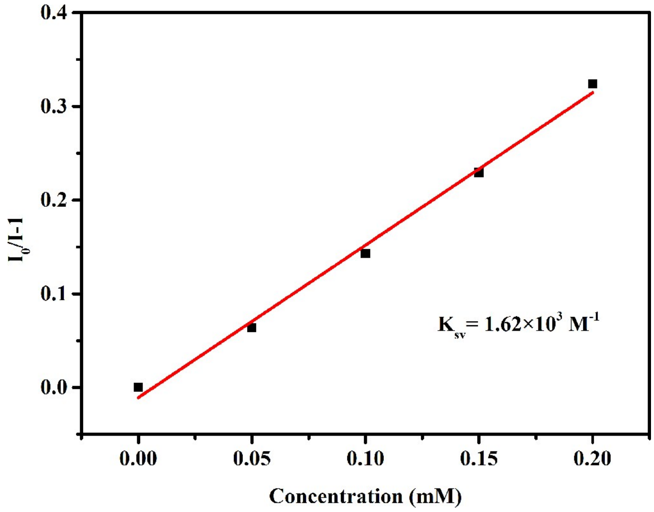

Figure S33. Stern-Volmer plot for NB of **2** in DMF suspension at the low concentration(0-0.2mM).

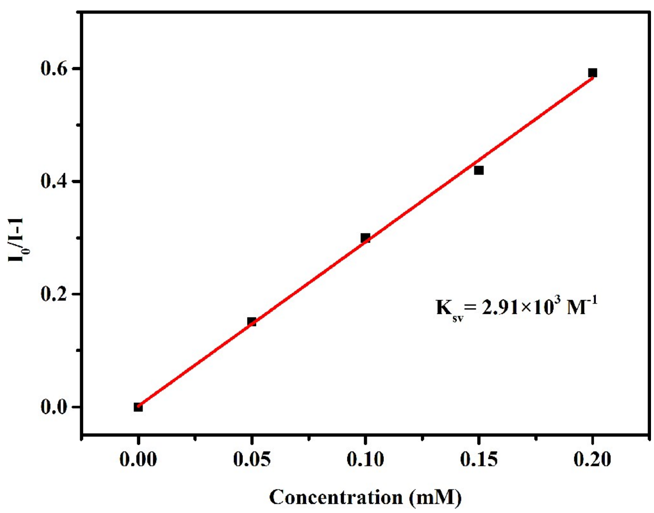

Figure S34. Stern-Volmer plot for *m*-DNB of **2** in DMF suspension at the low concentration(0-0.2mM).

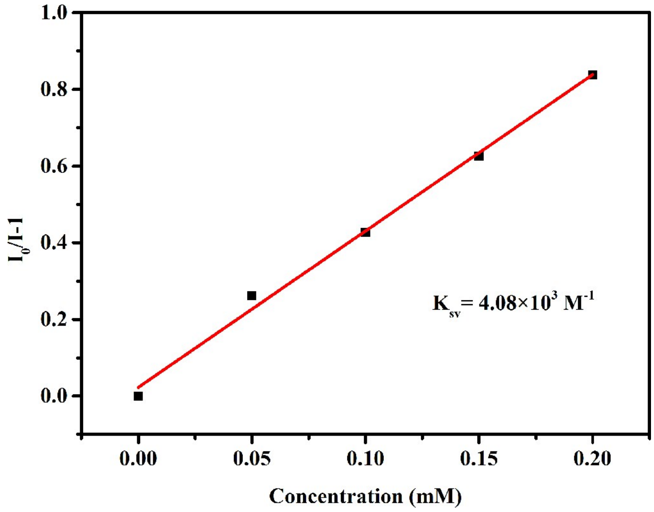

Figure S35. Stern-Volmer plot for 2,4-DNT of **2** in DMF suspension at the low concentration(0-0.2mM).

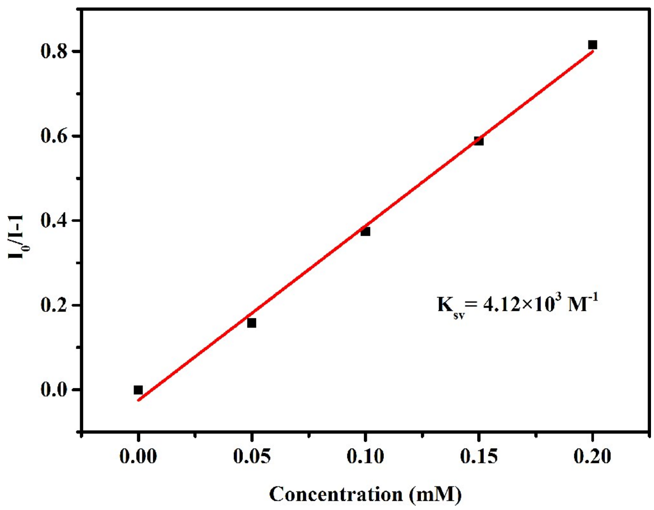

Figure S36. Stern-Volmer plot for PNT of **2** in DMF suspension at the low concentration(0-0.2mM).

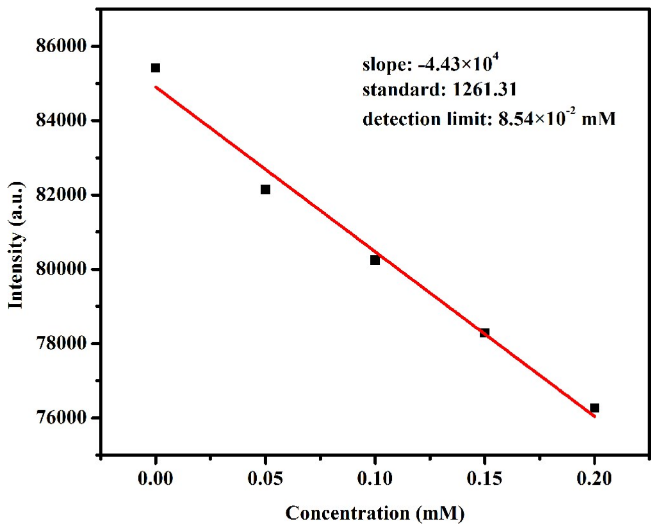

Figure S37. The detection limit for NB of **1** in DMF suspensionwas calculated with 3σ/k (k: slope, σ: standard) ina linear fitting range from 0 mM to 0.2 mM.

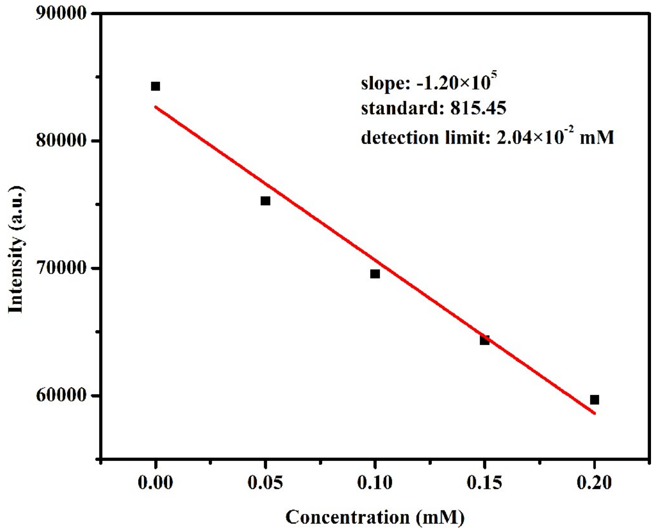

Figure S38. The detection limit for *m*-DNBof **1** in DMF suspensionwas calculated with 3σ/k (k: slope, σ: standard) ina linear fitting range from 0 mM to 0.2 mM.

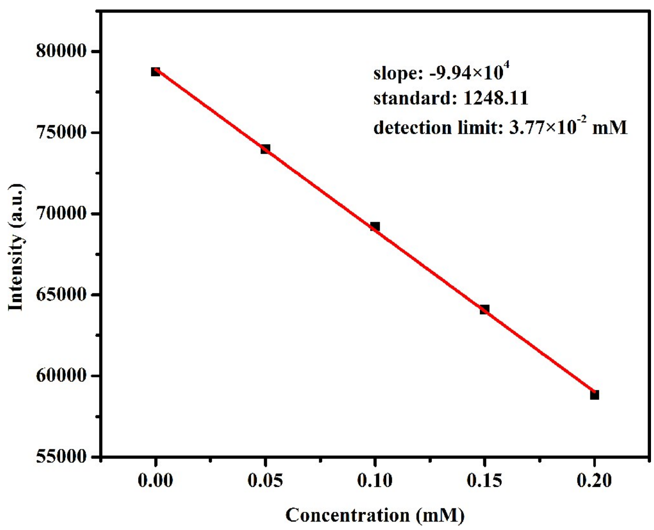

Figure S39. The detection limit for 2,4-DNTof **1** in DMF suspensionwas calculated with 3σ/k (k: slope, σ: standard) ina linear fitting range from 0 mM to 0.2mM.

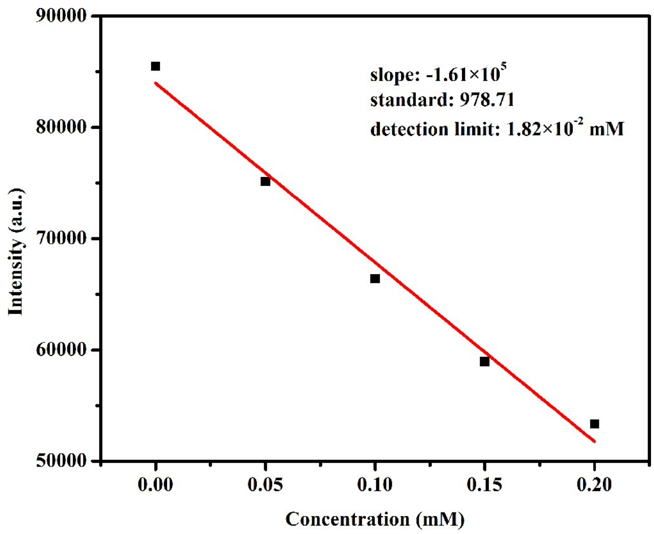

Figure S40. The detection limit for PNT of **1** in DMF suspensionwas calculated with 3σ/k (k: slope, σ: standard) ina linear fitting range from 0 mM to 0.2mM.

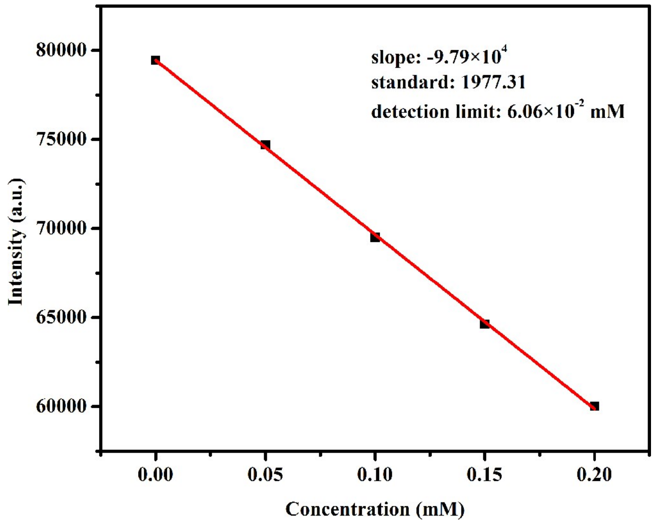

Figure S41. The detection limit for NB of **2** in DMF suspensionwas calculated with 3σ/k (k: slope, σ: standard) ina linear fitting range from 0 mM to 0.2mM.

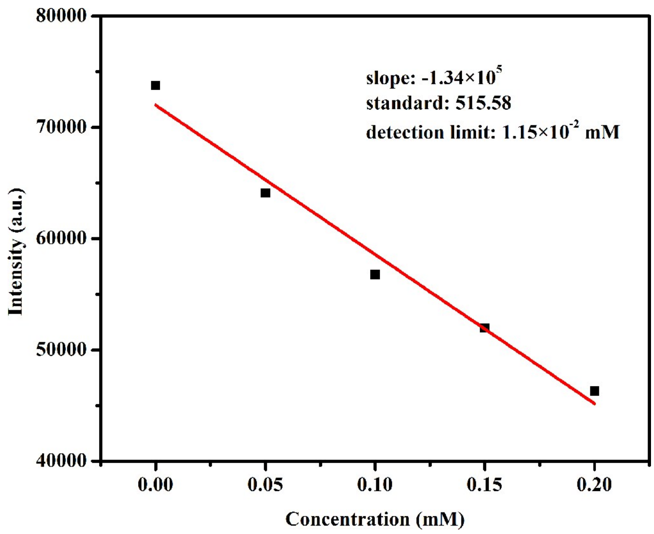

Figure S42. The detection limit for *m*-DNBof **2** in DMF suspensionwas calculated with 3σ/k (k: slope, σ: standard) ina linear fitting range from 0 mM to 0.2mM.

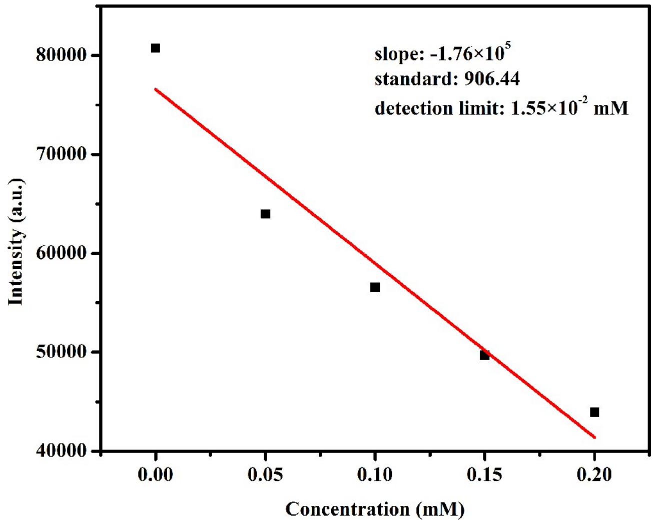

Figure S43. The detection limit for 2,4-DNTof **2** in DMF suspensionwas calculated with 3σ/k (k: slope, σ: standard) ina linear fitting range from 0 mM to 0.2mM.

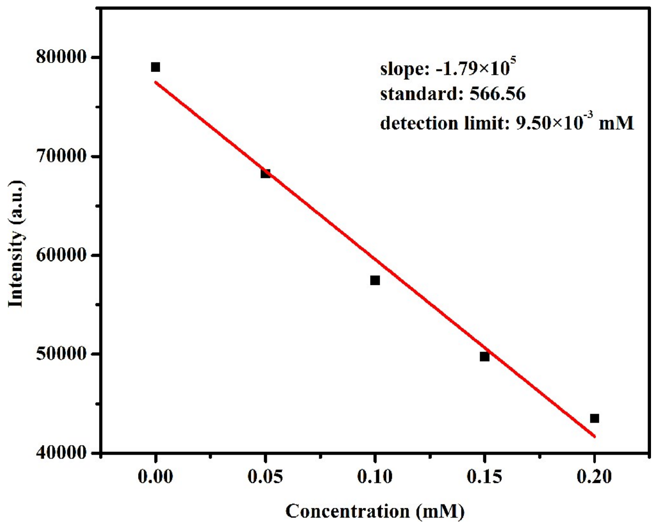

Figure S44. The detection limit for PNT of **2** in DMF suspensionwas calculated with 3σ/k (k: slope, σ: standard) ina linear fitting range from 0 mM to 0.2mM.

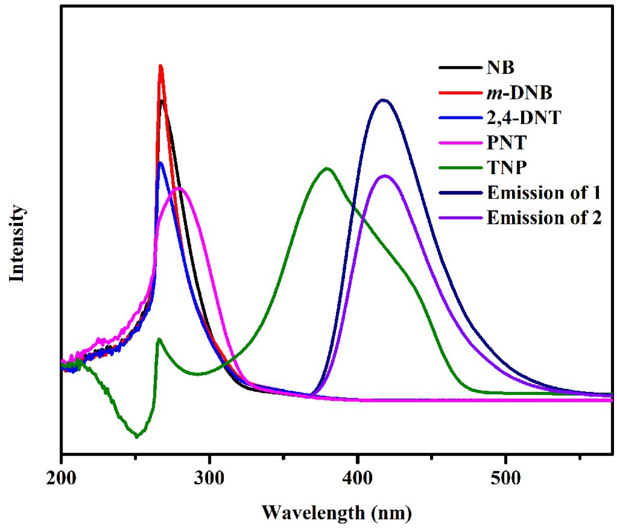

Figure S45. Spectral overlap between the absorption spectra of NB, *m*-DNB, 2,4-DNT, PNT, TNT and the emission spectra of **1** and **2** in DMF media.

TableS1 Selected bond lengths (Å) and angles (º) for **1**.

Zn(1)-O(1)	2.054(3)	Zn(2)-O(2)	2.025(4)
Zn(2)-O(3)#2	2.030(4)	Zn(1)-O(4)#2	2.049(4)
Zn(1)-O(5)#1	2.020(3)	Zn(2)-O(6)#1	2.025(3)
Zn(2)-O(7)	2.024(3)	Zn(1)-O(8)	2.031(3)
Zn(1)-N(1)	2.038(4)	Zn(2)-N(6)#3	2.030(4)
O(5)#1-Zn(1)-O(8)	159.24(15)	O(5)#1-Zn(1)-N(1)	98.40(15)
O(8)-Zn(1)-N(1)	102.35(15)	O(5)#1-Zn(1)-O(4)#2	89.66(17)
O(8)-Zn(1)-O(4)#2	87.15(16)	N(1)-Zn(1)-O(4)#2	100.57(15)
O(5)#1-Zn(1)-O(1)	86.80(17)	O(8)-Zn(1)-O(1)	88.20(17)
N(1)-Zn(1)-O(1)	102.32(14)	O(4)#2-Zn(1)-O(1)	157.11(15)
O(7)-Zn(2)-O(2)	87.59(17)	O(7)-Zn(2)-O(6)#1	157.79(15)
O(2)-Zn(2)-O(6)#1	87.25(17)	O(7)-Zn(2)-N(6)#3	98.66(15)
O(2)-Zn(2)-N(6)#3	100.36(14)	O(6)#1-Zn(2)-N(6)#3	103.52(15)
O(7)-Zn(2)-O(3)#2	89.29(16)	O(2)-Zn(2)-O(3)#2	159.65(14)
O(6)#1-Zn(2)-O(3)#2	88.08(16)	N(6)#3-Zn(2)-O(3)#2	100.00(15)

Symmetry transformations used to generate equivalent atoms: #1 x, -y+1/2, z-1/2; #2 x-1, y, z; #3 x, -y+1/2, z+1/2.

Table S2 Selected bond lengths (Å) and angles (º) for **2**.

Cd(1)-N(1)	2.268(2)	Cd(1)-N(8)#1	2.268(2)
Cd(1)-O(1)	2.419(2)	Cd(1)-O(2)	2.3492(19)
Cd(1)-O(3)#2	2.303(2)	Cd(1)-O(4)#3	2.327(2)
N(1)-Cd(1)-N(8)#1	174.91(9)	N(1)-Cd(1)-O(3)#2	83.77(9)
N(8)#1-Cd(1)-O(3)#2	91.28(9)	N(1)-Cd(1)-O(4)#3	92.27(8)
N(8)#1-Cd(1)-O(4)#3	90.20(8)	O(3)#2-Cd(1)-O(4)#3	132.48(8)
N(1)-Cd(1)-O(2)	95.43(8)	N(8)#1-Cd(1)-O(2)	89.25(8)
O(3)#2-Cd(1)-O(2)	143.38(7)	O(4)#3-Cd(1)-O(2)	84.12(7)
N(1)-Cd(1)-O(1)	85.14(8)	N(8)#1-Cd(1)-O(1)	95.93(8)
O(3)#2-Cd(1)-O(1)	88.35(7)	O(4)#3-Cd(1)-O(1)	138.64(7)
O(2)-Cd(1)-O(1)	55.22(7)		

Symmetry transformations used to generate equivalent atoms: #1 x, y, z+1; #2 -x-1, y-1/2, -z+1/2; #3 x-1, -y+1/2, z-1/2.